COBEM 2021 26th International Congress of Mechanical Engineering
ABCM Associação Brasileira de Engenharia e Ciências Mecânicas
November 22-26, 2021, Virtual Congress, Brazil

COBEM-2021-0143
TECHNICAL AND ECONOMIC ANALYSIS OF A SOLAR WATER HEATING SYSTEM TO AVOID THE FORMATION OF PARAFFIN DEPOSITS IN ONSHORE OIL PRODUCTION COLUMNS

Vinicius Rugeri Borges Bonini
vinicius.bonini@lepten.ufsc.br
Allan Ricardo Starke
allan.starke@lepten.ufsc.br
Sergio Colle
sergio.colle@ufsc.br
Laboratory of Energy Conversion Engineering and Energy Technology - Technological Center - Federal University of Santa Catarina - LEPTEN/CTC/UFSC.
Trindade, Florianópolis, SC, CEP 88040-900, Brazil.

Abstract. *The paraffin deposition on oil production columns, can cause some problems, incurring in financial losses, and even safety problems. To avoid pipe obstruction, hot water injection inside the production column can be done to solve this problem. The decision of replacing the conventional systems with a solar system requires a technical and economical evaluation of the behavior of the new system. The present work focused on the transient simulation to evaluate the performance of a proposed solar water heating system, by using TRNSYS software. The proposed system consists of a field of flat plate solar collectors, which heats the injection water indirectly through a coiled heat exchanger immersed in a thermal storage (*$3\ m^3$*). The heated water is injected daily into the oil production column. The simulation platform can consider the shading in the collector field and the pressure drop of the hydraulic circuit. For Candeias-Bahia, the effects of the design variables, collector area, slope, fuel tariff, inflation, and discount rate, on the thermal and economic performance of the system were analyzed. Optimization in terms of the analyzed variables, lead to an optimized LCS of R$151.900,00, a solar field of* $113.22\ m^2$*, an annual solar fraction of* $63,7\%$ *and 6.6 years of payback.*

Keywords: *Avoid paraffin deposition, petroleum, solar process heat, simulation, economic analysis, TRNSYS*

1. INTRODUCTION

The contemporary human lifestyle demands huge amounts of energy, used both for the basic necessities, as lightning and heating, and for production processes. Estimates point that until 2040 the energetic global demand, from primary sources, will grow 40% (OPEC, 2016). In 2019, the global primary energy was $602.27\ EJ$, of which, 31% ($188.91\ EJ$) were supplied by oil, 26% ($157.51\ EJ$) were by coal and 23% ($139.00\ EJ$) were by natural gas. In the other hand, the renewable sources contributed with 14%, showing a growth of 12.2% between 2018 and 2019 (IEA, 2019).

Nowadays the oil and gas industry is one of the greatest energy consumers, since, the processes related to the extraction and refining of the hydrocarbons demands huge amounts of energy (United Nations, 2012). The process of production and refining of oil, mostly demands lots of thermal energy, that, sometimes is supplied through the fuel being produced, that, accordingly to (Halabi *et al.*, 2015), corresponds to 10% of the fuel produced.

Aiming to better use the fossil fuels extracted, and to reduce the environmental impact caused by its processing, it is mandatory the reducing in the consumed fuel to supply the thermal energy demand of the processes. In this context, the use of Solar Heating for Industrial Processes (SHIP), shows great potential, once it reduces the use of fossil fuels and/or electricity as heat source for the processes, besides, result in lower greenhouse gasses emissions and environmental impacts. Furthermore, another advantage, is that, with less fuel being used to supply the production processes, more fuel is available to commercialization.

Among the various processes with thermal energy demands in the oil industry, in this work is going to be analyzed the the problem that exists in the crude oil extraction operations in oil production columns. According to Palermo *et al.* (2014) the problems related to the deposition and crystallization of heavy organic oil fractions during the production, transport and storage of crude oil may cause several losses to the oil industry.

Aiming to avoid the appearance of incrustation in oil production column, many solutions can be found in the literature. One of these solutions, to avoid this problem, is the periodic warming of the oil production column, through the injection of water heated to a temperature of $95°C$ in the external jacket of the production column. Since that, in the context of

the oil production column the process temperature is low, a SHIP solution can be used. Another advantage that must be highlighted, is that this system has low complexity and it is easy to replicate in other oil production wells.

In this context, the main objective of this paper is to propose a water heating SHIP system to attend the thermal demand required, to prevent the occurrence of paraffin deposition in the oil production column. This system must heat the water indirectly, considering the pressure drop of the fluid through the hydraulic frame, the self and external shading in the solar field, and of a passive cooling system to protect the system. In this context, it is going to be developed a transient simulation platform, to design the system and to assess its technical and economical behavior.

2. LITERATURE REVIEW

The crude oil is a complex hydrocarbons mixture, divided in different groups, as paraffins, aromatics, naphthenes, resins and asphaltenes (Singh *et al.*, 2000; Palermo *et al.*, 2014; Bai and Zhang, 2013), the three main components being aromatics, naphthenics and paraffins (Davies, 2002).

This crude oil is extracted from underground and underwater reservoirs, which are at temperatures on the order of $70°C$ to $150°C$, and pumped to the surface through pipelines. The pipelines are in contact with an external environment at a temperature lower than that of the well, thus, they cool the crude oil (Singh *et al.*, 2000). The cooling of the crude oil results in a crystallization process and deposition of the paraffin existing in the hydrocarbons mixture in the pipe walls through which the fluid is flowing (Palermo *et al.*, 2014). The formation of paraffin layers in the pipe walls ends up restricting the flow of crude oil, reducing the production efficiency, may causing emergency stoppages and even safety problems (Singh *et al.*, 2000; Liu *et al.*, 2015; Cheng *et al.*, 2017). The physical mechanisms proposed to explain the paraffin deposition in the pipe walls are presented by Singh *et al.* (2000), and are not scope of the present work.

In underwater pipes, oil pipelines and wells, the costs of controlling and correcting unforeseen problems arising from paraffin deposition are substantial (Brown, 1993). Currently the removal of paraffin deposition generates a lot of expenses (Liu *et al.*, 2015), the magnitude of this problem can be seen through the example of the Lasmo Company (United Kingdom), which had to abandon a platform at a cost of US$100 million due to problems with the deposition of wax in the pipes (Singh *et al.*, 2000; Venkatesan *et al.*, 2005).

Among the means of correcting the problem of paraffin, the replacement of the affected pipe segment is the procedure used in situations of severe blocking of the cross section (Venkatesan *et al.*, 2005), which results in high operating costs. In less severe situations another way of correcting the problems arising from the paraffin deposition is the mechanical pigging, which consists of scraping the paraffin deposits from the pipe, being the most used method for removing paraffin wax deposits in pipes (Venkatesan *et al.*, 2005). Another solution is the fusion of the paraffin deposit using a thermal source, as a chemical reaction, electrical heating or heat injection in the affected pipe (Nguyen *et al.*, 2001; Chi *et al.*, 2019).

Besides the three solutions cited, many other methods can be found in the literature, mainly in the work made by Chi *et al.* (2019), where is presented a concise literature review of the solutions used in the oil and gas industry. Although the problem of paraffining is more frequent and more expressive in offshore sites, this problem also occurs in oil and gas exploration in onshore stations. Thus, the present work will deal with the deposition of paraffin wax in onshore installations.

As explained, one method to avoid the formation of paraffin deposits is the heat injection in the pipe. In this context, it was proposed a method that consist in maintaining the oil production column always heated, with this heating being carried out through the daily injection of hot water into the production column. The latter being the object of study of this work.

3. METHODOLOGY

The conceptual design of the solar water heating system, to attend the heating demand is presented schematically in Figure 1. The system must operate on a close loop with indirect heating of the injection water, through an immersed heat exchanger inside the storage, The heat exchanger is composed of 20 pipes, with $11.36\ m$ length each, with an inside diameter of $26.64\ mm$, and an external diameter of $33.40\ mm$. The use of the immersed heat exchanger is due to the possibility of using different heat transfer fluids in the hydraulic circuit of the collectors, for example, raising the boiling temperature of water.

In the default design, the solar field has 50 solar collectors, with a slope of $12.67°$, arranged in five parallel rows, with ten collectors each, corresponding to an area of $94.35\ m^2$, and a HTF flow rate of $1\ kg/s$. There is a heat sink in the hydraulic frame, designed to dissipate $60\ kW$, with 6 tubes of $2.8\ m$ length each. This component works as a protection device for the system, avoiding reaching and operating at temperatures close to the stagnation stagnation, preserving the integrity of the system, as recommended by Frank *et al.* (2015). The meteorological data used correspond to the city of Cruz das Almas, Bahia, Brazil.

The system is design to do a daily injection of heated water at $95°C$ in the production column, scheduled to happen at 3 p.m. The thermal storage has a volume of $3\ m^3$, an aspect ratio of $1/3$ and an auxiliary heating system of $30\ kW$.In

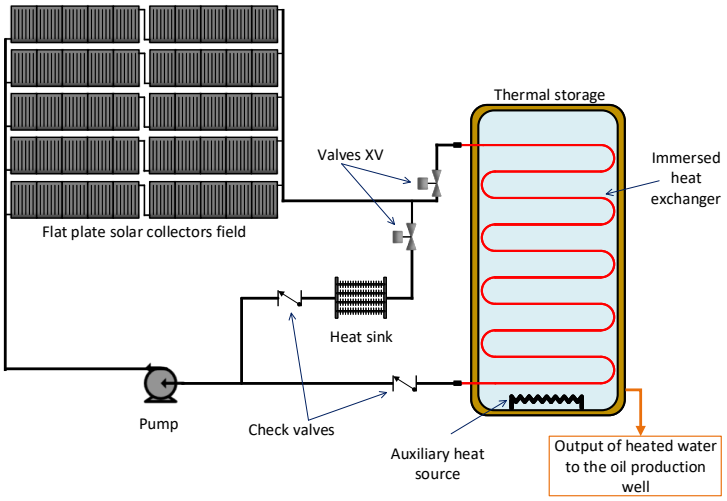

Figure 1: Conceptual design of the solar water heating system.

this sense, daily, at 3 p.m., the control system verifies the mean storage temperature, if it is equal or greater to $95°C$ (injection temperature), than, the HTF[1] flow is diverted to the heat sink, and the whole storage's heated water is injected in the production column. In other hand, if the storage's mean temperature is below $95°C$, the auxiliary heating system is activated, and works until the injection temperature is reached, while the HTF flows through the heat sink. When the storage's mean temperature is equals to the injection temperature, the injection is done. Is important to point out, that is scheduled one injection daily, not being allowed more than one injection. After the injection, the storage is filled with water unheated, and the HTF returns to flow in the immersed heat exchanger, restarting the storage's water heating, if, of course, there is enough solar energy available in the solar field.

Based on the conceptual design of the solar water heating system and the control strategy, it is proposed a simulation model in the TRNSYS simulation environment. The software TRNSYS has a generalized simulation, developed to simulate the transient behavior of systems, with its main focus being the simulation of thermal systems, having a modular and open-source structure. The tool works with modular components, called types, that are consolidated mathematical models that represents the physical behavior of the equipment.

The construction of a project within the TRNSYS graphic environment starts with the selection of the types that will represent the system components, in this sense, in the next subsection, a brief explanation will be made.

3.1 Simulation Components

The explanations of the simulation components used in this work are presented in this section. Concerning the model that accounts the pressure drop across the straight pipes using the Darcy-Weisbach equation. Regarding the pressure drop across accessories and valves, they are accounted based on the models described by Idelchik (2008).

The component that represents the pump, has constant velocity, maximum flow rate specified by the user, controlled by an external control function. The power consumed by the component can be calculated by a linear function between power and mass flow, or by a relationship provided by the user.

The set of meteorological data used for the simulations is called the typical meteorological year, (TMY - Typical Meteorological Year), which gathers the average meteorological conditions of the locality for a period of 30 years (Duffie and Beckman, 2013). In Brazil there are three main sources of solar radiation data: the SWERA project database (Solar and Wind Resource Assessment), the SONDA network stations and the data from INMET meteorological stations. For the present study, the climate data for the city of Cruz das Almas state of Bahia, where there is an automatic INMET station.

The solar radiation data from the INMET stations comprise only the total incident radiation (sum of the direct portion and the diffuse portion), without the necessary detail to carry out the simulations, that is, the direct radiation and diffuse solar radiation incident on the horizontal plane (Lemos *et al.*, 2017). In order to solve this problem, models can be used to determine the incident direct radiation. Among the available models, the BRL-Brazil model was used. This model is an evolution of the Boland-Ridley-Laurent (BRL) model, which was adjusted to the characteristics of the Brazilian climate, with the full description of the model available in the work of Lemos *et al.* (2017).

The flow in the rows of collectors must be balanced in order to keep the outlet temperature of each one of the rows constant. In order to carry out this balance, the diameter of the head tubes must be scaled to maintain the velocity of the thermal fluid flow relatively constant (Wagner and Gilman, 2010). The scaling was performed following the methodology

[1]Heat transfer fluid, in the present case is water.

described by Wagner and Gilman (2010), for the inlet and output header, with a minimum speed of $2m/s$, and a maximum speed of $3m/s$ (Kelly and Kearney, 2006).

The mathematical model that represents the insulated pipes consider a pipe with constant diameter, where there is a series of fluid elements, completely mixed, and interconnected, with thermal insulation, which exchange heat with the external environment through the radiation emitted by the surface and natural or forced convection, with the user being responsible for determining which type of convection exists in his simulation. The component's thermal model also considers the effects of thermal insulation mass and pipe material on the energy balance of the component (TESS, 2012a). The pressure drop in a straight pipe is calculated using the Darcy-Weisbach equation.

The thermal storage can be divided into uniform temperature elements in order to model the existing stratification in storage tanks, with the user being able to control the degree of stratification by selecting the amount of stratified elements, in addition to allowing auxiliary heating via electrical resistance. The design of the heat exchanger inside the storage is done by selecting its type, internal diameter, external number of tubes, and the correlation of convection inside the reservoir (between water and heat exchanger) (TESS, 2014).

The heat sink is composed of a set of finned tubes in parallel, which exchange heat either by natural convection or forced convection with the external environment. The heat sink sizing uses as input parameters the thermal power to be dissipated under design conditions, the fin dimensions and the pipe diameters. The length of the heat sink tubes is determined in order to guarantee that, in the design condition, the thermal exchange is equal to the required thermal power. With the heat sink length determined, transient operation of the component is performed.

The thermal exchange between the hot fluid flowing in the finned heat sink tubes and the environment occurs through forced convection between the fluid and the inner walls of the pipe, by conduction through the finned tubes, and by mixed convection between the outer surface of the tubes and the external environment. To determine the length of the heat sink tubes a discrete iterative procedure was implemented, by joining elementary segments of finned tubes of fixed length.

The flat plate collectors model considers that the collectors are mounted in series and parallel, considering the effects of the thermal capacitance of he HTF inside the collector. The efficiency of the collectors is based on the difference between the fluid inlet temperature and the ambient temperature (TESS, 2012b).

The passage of the thermal fluid through the heat sink is controlled by a thermostat designed for cooling systems. This component works with hysteresis to avoid instability problems when the measured temperature is close to or equal to its set-point. For the auxiliary heating/water injection system and to prevent overheating of the collectors, a temperature controller with minimum operating time was used.

The collector pump is controlled by a differential temperature controller with hysteresis and minimum activation time, that is, when activated there is a minimum time that the collector pump must be activated.

The auxiliary heating and the injection of heated water depend primarily on the time of day, since it is a premise of the system that the injection takes place essentially from 3 pm daily, except in cases where the reservoir temperature reaches the injection temperature before 3 pm.

4. RESULTS AND DISCUSSION

The results obtained for the simulation of the system implemented in TRNSYS are presented in the sequence. Firstly, it is described how the simulation occurs, in one day of the system operation, as well as the presentation of the thermo-economic results obtained for the default case. In the sequence, the sensitivity analyzes in terms of parameters of interest are presented, namely, the number of rows in the collector field, the slope of the collectors, cost of the sources of auxiliary energy, fuel inflation rates and discount rate.

4.1 Daily operation of the system

The detailed operation of the system is shown and explained in Figure 2, where the operation of one day is shown, in which the system performed the injection before 15:00, since it stored enough energy to reach the injection temperature before the scheduled time stipulated. In addition, on the present day, there was no need for auxiliary heat input, as it was possible to perform an injection before the specified time.

In Figure 2, the solid green line represents the immersed heat exchanger outlet temperature ($T_{out,HX}$), the blue line represents the collector field inlet temperature ($T_{in,col}$), the cyan line represents the collector field outlet temperature ($T_{out,col}$), the red line is the heat sink inlet temperature ($T_{in,sink}$), the pink line symbolizes the heat sink output temperature ($T_{out,sink}$), the purple line corresponds to the average temperature of the storage ($T_{avg,sto}$), and the solid gray line refers to the ambient temperature (T_{amb}). At the bottom, referenced to the right ordered axis, entitled Flow kg/h, we have the lines that represent the mass flow, with the dotted light blue line referring to the mass flow in the collectors and the immersed heat exchanger ($\dot{m}_{serp}$), the orange dashed line corresponding to the mass flow in the heat sink ($\dot{m}_{sink}$) and the dashed green dot line being the flow in the reservoir ($\dot{m}_{storage}$), that is, the occurrence of the injection.

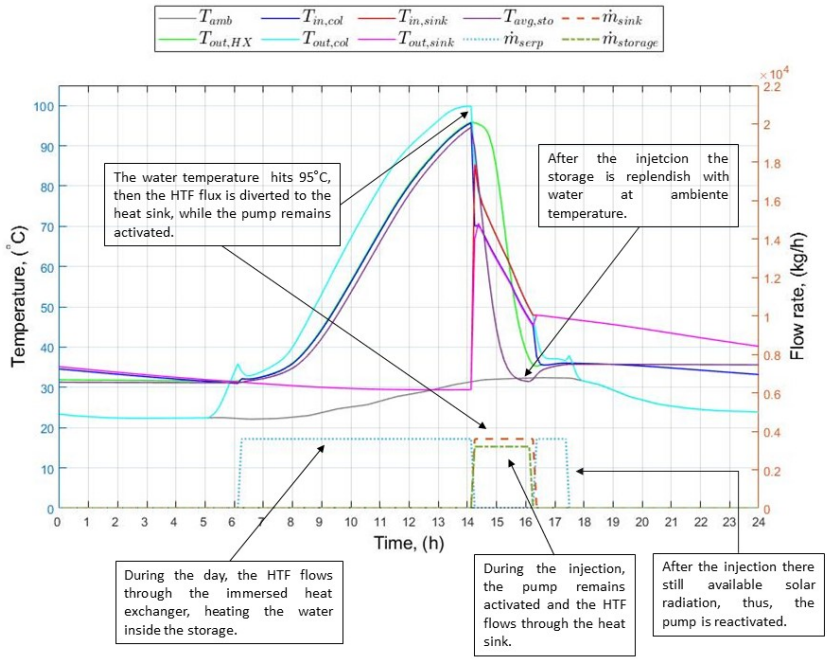

Figure 2: Daily system operation for a day with high solar radiation.

4.2 Default case

The default case is defined based on the parameter presented in Section 3, and the system shown in Figure 1. Aiming to verity how the system operates yearly for the default case, in Figure 3a the main energies monthly average daily value[2] that exists in the systems are presented.

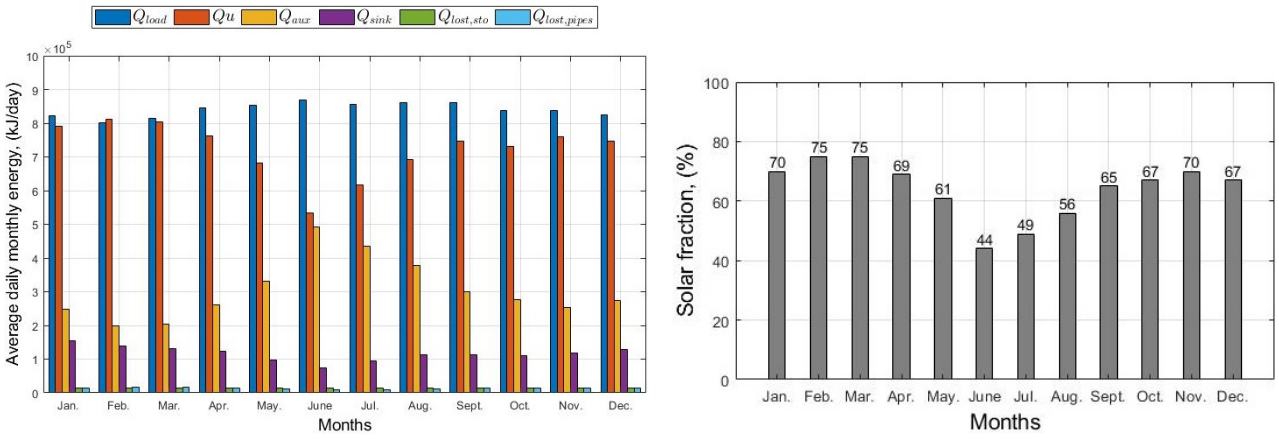

(a) Average Monthly energies for the solar water heating system. (b) Solar fraction for the solar water heating system.

Figure 3: Monthly results for the system.

It can be seen in Figure 3a that the energy delivered for demand (blue bars - Q_{load}) remains approximately constant during the year, having a small increase during the months of June, July, August and September, when the ambient temperature is lower. On the other hand, the thermal gain of the collectors (red bars - Qu) drops drastically for the same months. Proportionally with the drop in the gain of the collectors, the auxiliary energy (yellow bars - Q_{aux}) increases for the winter months, in order to meet the thermal demand. Regarding the dissipated energy (purple bars - Q_{sink}), it is higher for the months when the collector gain is higher. The thermal losses of the reservoir (green bars - $Q_{lost,sto}$) and pipes (light blue bars - $Q_{lost,pipes}$) remain approximately constant during the year, with small values compared to the other energies of the system.

In a complementary way, in Figure 3b the monthly solar fraction of the system is presented. Solar fraction is a performance indicator commonly used to describe performance of a solar system. This performance indicator represents

[2]Integral monthly energy divided by the number of days of the month $\frac{\int^N Q\ dE}{N}$

the percentage of energy demand that was supplied by the solar system, with the remainder of the demand being supplied by the auxiliary energy source (Duffie and Beckman, 2013). As expected, the solar fraction of the system is lower for the months of June, July and August, winter months, reaching a minimum of 44% for the month of June. For the other months of the year, the system has a solar fraction above 60% for every month, reaching a maximum of 75% in February and March. Resulting in an annual solar fraction of 63.7%.

Regarding the pressure drop, the maximum value obtained was $207.22\ kPa$, requiring a pump of $224.41\ kW$ of electric power, with efficiency pumping rate of 95%. For one year of system operation, it has been determined that this pump will consume $1.08\ MWh$ of electrical energy.

For the economic analysis, two distinct economic scenarios were analyzed, the first is the replacement of a system that uses gas as an energy source, by a solar system that uses gas as an auxiliary energy source. And the second case, using electricity as an auxiliary heating source. The rate of future change in the electricity was determined through the historical analysis of the rate of change in fuel prices, based on data obtained on the ANEEL website ANEEL (2019) ($i_g = 6.0\%$), for a period of 10 years (2009 to 2019), the rate of change in the price of natural gas (inflation) was taken from Starke *et al.* (2017) ($i_e = 5.0\%$). The fuel[3][4] and solar collector costs[5] were taken from Solar Payback (2018) and the thermal storage cost[6] from Mauthner and Herkel (2016). To estimate the cost of the heat sink, a survey of the finned tube cost per unit length was carried out. This cost was multiplied by a correction factor to account for additional costs associated with component manufacturing (pipe arrangement, assembly, pipe support, etc.), resulting in $C_{sink} = R\$\,16,000.00$.

Louvet *et al.* (2017) suggests that the weighted average cost of capital (WACC) be used as the discount rate for economic analysis. According to Rocha *et al.* (2012), the average WACC, excluding inflation, for renewable energy in Brazil is 9.43%. The annual operating and maintenance costs were1.0% of the initial investment, as suggested by Solar Payback (2018), without inflation. The economic analysis was performed for a period of 20 years as suggested by Starke *et al.* (2017); Solar Payback (2018); Cardemil *et al.* (2018).

The economic criteria analyzed refers to LCS, payback time and ROI. For the electricity case the performed LCS is $R\$\,144,163.10$, the payback times is 6.6 years and the ROI is 15.1%. For the natural gas case, the LCS is $-R\$\,103,238.93$, the payback times is 21.9 years and the ROI is 4.6%. Analyzing the economic results, it is clear that the most favorable scenario occurs for the exchange of an electrical system for a solar/electric system, and the least advantageous, presenting financial loss, is the replacement of the system to gas by a solar/gas system. The fact that the electricity scenario is more favorable is due to the fact that the cost of electricity is higher than the cost of gas, for this same reason the gas scenario becomes disadvantageous.

4.3 Parametric analysis

Among all the input parameters for system simulation, five parameters of interest were selected to verify the system's sensitivity to them. The selected variables were: the number of rows in the collector field, the slope of the collectors, the tariff of the auxiliary energy source, the rate of change in future fuel price (inflation) and the discount rate.

4.3.1 Rows in the collector field

The first parametric analysis performed was the variation of the collector field area, keeping the number of collectors per row constant, adding the rows, from 2 rows to 13 rows. The flow through the system was changed according to the amount of collectors present. Figure 4a shows the annual solar fraction of the system as a function of the collector field area. As expected, the addition of the solar field area raises the solar fraction of the system asymptotically.

In order to verify the savings promoted by the replacement of conventional systems by the solar system, Figure 4b presents the two LCS scenarios evaluated within the parametric analysis, where the line with squares represents scenario 1, (LCS_{gas}) and the line with circular markers represents scenario 2, (LCS_{ele}). From Figure 4b, it is clear that the best economic scenario, with the highest economic return is for the electric case, with a maximum point of $R\$\,151,000.00$ for the LCS_{ele}, corresponding to the area of $113.22\ m^2$. The LCS_{gas}, for all areas analyzed, resulted in a loss, with the solar solution proving to be economically unfeasible.

4.3.2 Slope of the collectors

The slope of the collectors is a parameter that directly impacts their thermal gain (Duffie and Beckman, 2013). Furthermore, the slope of the collectors also interferes with the shading between the rows of collectors in the solar field. Thus, a parametric analysis of the slope of the collectors, (β), from $0°$ to $40°$ was performed. The solar fraction, and the shading factor between rows of the collector field, as a function of the slope of the collectors, are presented in Figure 5a.

[3] $C_{gas} = 164.00\ R\$/Mwh$
[4] $C_{ele} = 535.25\ R\$/Mwh$
[5] $C_{collector} = 1,323.00\ R\$/m^2$
[6] $C_{storage} = 6,187.0\ R\$/m^3$

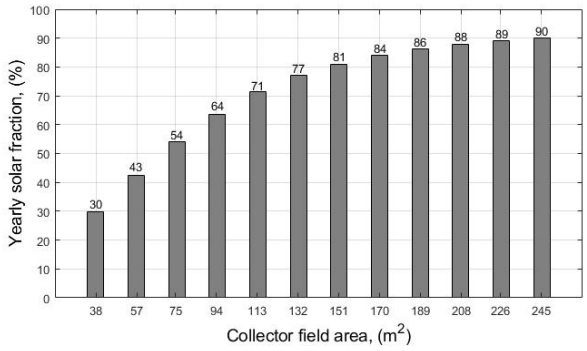

(a) Yearly solar fraction as a function of the solar field area.

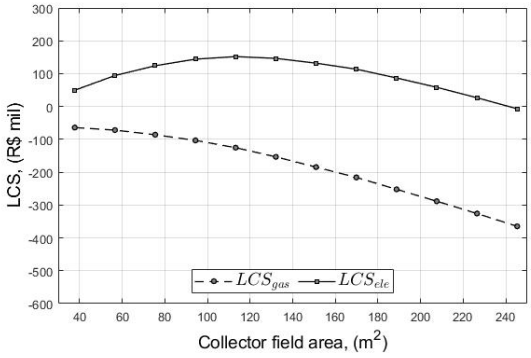

(b) LCS as a function of the solar field area.

Figure 4: Results for the parametric analysis of the area.

The shading factor is calculated as the ratio of the difference between the total radiation incident on the first row and the second row (shaded), by the total radiation incident on the first row.

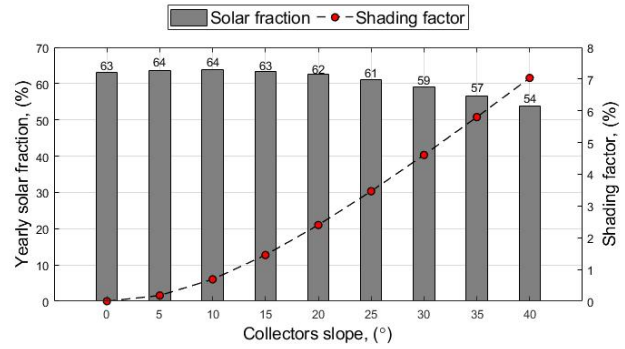

(a) Yearly solar fraction an shading factor as a function of the collectors slope.

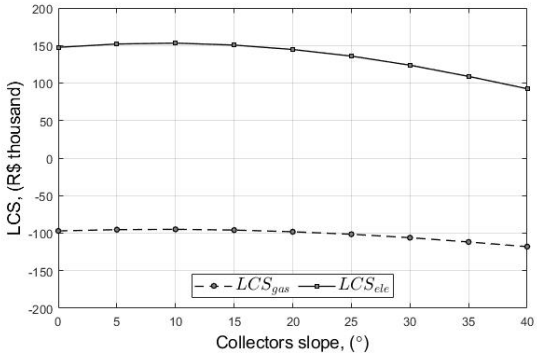

(b) LCS as a function of the collectors slope.

Figure 5: Results for the parametric analysis of the collectors slope.

Through Figure 5a, it is verified that the solar fraction decreases with the increase of the slope of the collectors, while the shading factor increases. The solar fraction has its maximum between $5°$ and $10°$, while the shading factor (dotted line) for the slope of $40°$, comes to 7%. In order to verify the influence of the slope on the economic analysis, Figure 5b presents the two scenarios of LCS as a function of the slope of the collectors.

It can be seen that the increase in the slope of the collectors results in an increase in the LCS up to the optimum point of $R\$\,145,000.00$, for the slope of $10°$, from which a reduction occurs. for both LCS, however, this behavior is more pronounced for LCS_{ele}. Despite the perceived reduction of LCS in Figure 5b, for the analyzed latitude, shading does not significantly affect system performance.

4.3.3 Tariff of the auxiliary energy source

An important economic parameter to be considered in a sensitivity analysis is the value of the tariff used for auxiliary energy sources. Figure 6a illustrates the behavior of LCS_{gas} and LCS_{ele} as a function of the rate variation fraction $C_{fuel}/C_{fuel,ref}$

The variation of the tariff is performed from 30% up to twice the original values. In Figure 6a there is a sharp increase in LCS_{ele}, which for the reference case was $R\$\,144,000.00$, for the twice higher rate, it had a profit of $R\$\,535,000.00$. The LCS_{gas} grows more smoothly, earning a profit starting in the rate of 1.7 times the initial adopted tariff, reaching a profit of $R\$\,40,000.00$ for the rate 2 times higher.

4.3.4 Rate of change in future fuel price

The rate of change in the future fuel price corresponds to the percentage rate at which fuel prices increase. Thus, the sensitivity of LCS as a function of the rate of change in fuel prices is presented in Figure 6b, and the two studied LCS scenarios are presented.

The increase in the rate causes an increase for both scenarios of the LCS, this occurs because the series of future

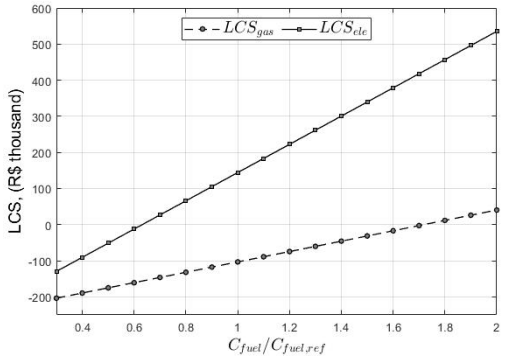

(a) LCS as function of the tariff of the auxiliary energy source.

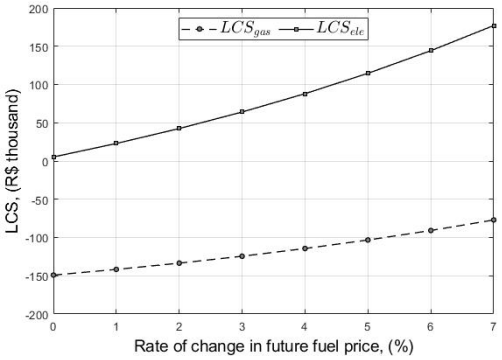

(b) LCS as function of the rate of change in future fuel price of the auxiliary energy source.

Figure 6: Results of the economic analysis.

fuel payments, are increased by the estimated percentage of inflation. Analyzing the LCS_{ele}, it can be seen that for the inflation of 0% its value is close to zero, whereas for the rate of 7% the LCS_{ele} was $R\$\,175,000.00$. The LCS_{gas} also increased with inflation, however, for the analyzed range, it did not result in profit.

4.3.5 Discount rate

The discount rate is an economic indicator that represents the minimum expected return on a given investment. This rate depends on market conditions, therefore, it is important to evaluate the behavior of the LCS against variations in this rate. It is verified, through the Figure 7a, that the discount rate significantly influences the system's LCS, especially the LCS_{ele}, which for a rate of 3.5% was $R\$\,490,000.00$, fell to a loss of $R\$\,89,000.00$ for the discount rate of 15.5%. With the rate of 3.5% it was possible to obtain a profit of $R\$\,45,000.00$ for the LCS_{gas}, however, for the other discount rates the system presents a negative LCS.

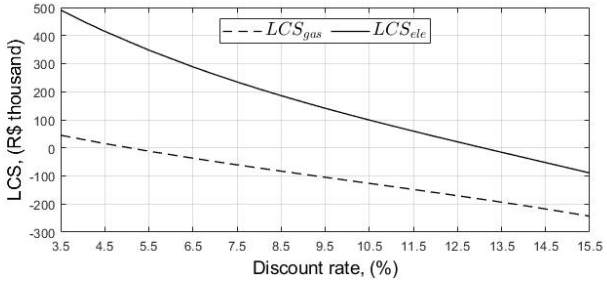

(a) LCS as a function of the discount rate.

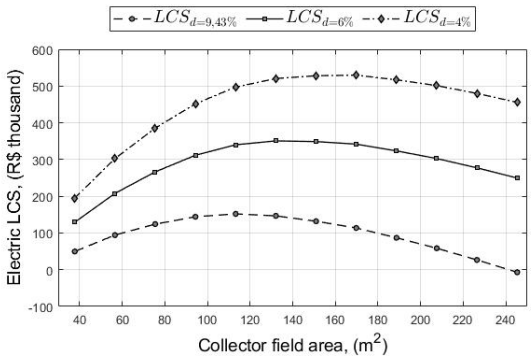

(b) Electric LCS as a function of the collector field area for three different discount rates.

Figure 7: Results of the economic analysis.

Since the electrical system showed economic viability in the preceding analysis, and in order to visualize the sensitivity of the LCS to the discount rate, a parametric analysis of the electrical LCS was performed as a function of the collector field area for 3 distinct discount rates, as shown in Figure 7b.

Higher discount rates actually reduce the system's LCS, for example, for the $94.35\ m^2$ area, the 4% rate generated a LCS of $R\$\,451,000.00$, whereas for 6% the LCS was $R\$\,311,000.00$, a reduction of 31%. It is verified that the areas that obtained the best results of LCS changed, for the rate of 4% the area of $169.83\ m^2$ resulted in the LCS optimal of was $R\$\,529,000.00$, whereas for the 6% rate, the area of $132.09\ m^2$ realized $R\$\,350,000.00$ of LCS.

Figure 8a presents the parametric analysis of the payback time as a function of the area of the collector field, for the discount rates of 9.43%, 6% and 4%, and the electrical system is again analyzed, given its economic viability.

The shortest payback time occurs for the areas $75.48\ m^2$ and $94.35\ m^2$ at all discount rates, with the minimum obtained being 5.5 years for the rate of 4%. Another economic criterion evaluated refers to the ROI, presented in Figure 8b. In terms of ROI, the most attractive system is the one with the highest value. Thus, the best case occurs for the area of 75.48 m^2, reaching 18.3%, with the reference area of $94.35\ m^2$ with the second best ROI, from 18.2%. There is a change from

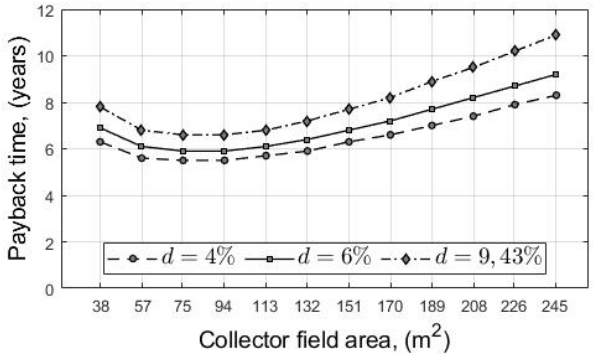

(a) Payback time as a function of the collector field area for three different discount rates.

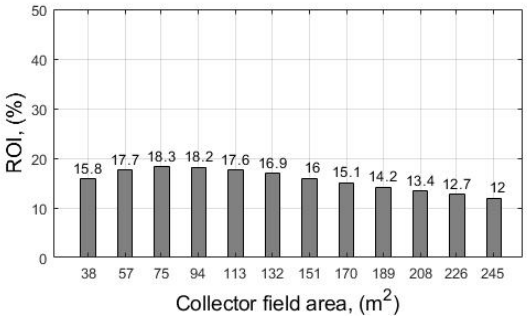

(b) ROI as a function of the collector field area.

Figure 8: Results of the economic analysis.

the area with the highest LCS to the area with the highest ROI. Generally speaking, economic scenarios in which gas was replaced by a solar system and gas-fired solar heating proved to be economically unattractive. On the other hand, the systems that consider the replacement of an electrical system by a solar system aided by electrical heating, showed economic viability for the analyzed parameters.

5. CONCLUSION

The objective of the present work was to propose a solar water heating system to meet a thermal process heat demand to avoid the formation of paraffin deposits in the oil production column, located in the city of Candeias in the state of Bahia, building a transient simulation platform to scale and analyze it. The simulation platform considers the shading between rows of the collector field, the pressure drop of the thermal fluid in the system, indirect heating of the thermal reservoir, and a heat sink used to protect the heating system.

The default case and resulted an annual solar fraction of 63.7%. For an analysis period of 20 years, the replacement of an electrically powered system with a solar heating system resulted in a cost of living savings of $R\$\,144,000.00$ and a payback time of 6.6 years. The system's sensitivity analysis to the design parameters showed that the slope of collectors had little influence on the economic result of the system for the analyzed latitude, with the optimal slope corresponding to $10°$, resulting in a LCS_{ele} of $R\$\,145,000.00$. Regarding the area of the collectors field, it was found that the largest LCS_{ele}, of $R\$\,151,000.00$, occurs for an area of $113.22\ m^2$, obtained for six rows of 10 collectors, mounted in parallel. The economic parameters analyzed were fuel tariff, fuel inflation and discount rate. The increase in the value of the fuel tariff and the fuel inflation rate caused an increase in the LCS, on the other hand, the increase in the discount rate caused a considerable drop in the LCS. For the electric case, the rate of 3.5% resulted in a LCS of $R\$\,490,000.00$ while the rate of 15.5% produced a loss LCS of $R\$\,45,000.00$. In addition to the results obtained and the analyzes carried out, the developed platform allows its user to carry out different thermo-economic analyzes of the implemented system, as well as of different system concepts and thermal demands. In addition, the tool is an important resource for evaluating and sizing the solar heating system. The system presented and simulated is already economically viable, however, it is vital to emphasize that the adoption of the solar system prevents the occurrence of blockages in the production column, which cause production stoppages. To remedy this problem, an expensive column cleaning procedure is required. As the solar system avoids this inconvenience, this avoided cost represents another form of economic benefit for the system under analysis.

6. ACKNOWLEDGEMENTS

The present work was developed with the support of the CNPq (Conselho Nacional de Desenvolvimento Científico e Tecnológico), through the process GM/GD - *Cotas do Programa de Pós-Graduação*, number 161586/2018-0, and PETROBRAS through the project 4600536881.

7. REFERENCES

ANEEL, 2019. "ANEEL". URL `https://www.aneel.gov.br/`.

Bai, C. and Zhang, J., 2013. "Thermal, macroscopic, and microscopic characteristics of wax deposits in field pipelines". *Energy and Fuels*, Vol. 27, No. 2, pp. 752–759. ISSN 08870624. doi:10.1021/ef3017877.

Brown, T.S., 1993. "Measurement and Prediction of the Kinetics of Paraffin Deposition". pp. 353–368.

Cardemil, J.M., Starke, A.R. and Colle, S., 2018. "Multi-objective optimization for reducing the auxil-

iary electric energy peak in low cost solar domestic hot-water heating systems in Brazil". *Solar Energy*, Vol. 163, No. March, pp. 486–496. ISSN 0038092X. doi:10.1016/j.solener.2018.01.008. URL https://doi.org/10.1016/j.solener.2018.01.008.

Cheng, C., Jia, W., Hei, D., Wei, Z. and Wang, H., 2017. "Feasibility study for wax deposition imaging in oil pipelines by PGNAA technique". *Applied Radiation and Isotopes*, Vol. 128, No. January, pp. 171–174. ISSN 0969-8043. doi:10.1016/j.apradiso.2017.07.017. URL http://dx.doi.org/10.1016/j.apradiso.2017.07.017.

Chi, Y., Yang, J., Sarica, C. and Daraboina, N., 2019. "A Critical Review of Controlling Paraffin Deposition in Production Lines Using Chemicals". *Energy and Fuels*, Vol. 33, No. 4, pp. 2797–2809. ISSN 15205029. doi:10.1021/acs.energyfuels.9b00316.

Davies, J.F., 2002. "Crude Oil". In A.G. Lucas, ed., *Modern Petroleum Technology – Volume 2: Downstream*, John Wiley & Sons Ltd, chapter Crude Oil, p. 488. 6th edition. ISBN 978-0-470-85022-0.

Duffie, J.A. and Beckman, W.A., 2013. *Solar Engineering of Thermal Processes, 4th ed.*, Vol. 116. ISBN 9780470873663. doi:10.1115/1.2930068. URL http://solarenergyengineering.asmedigitalcollection.asme.org/article.aspx?articleid=1455382.

Frank, E., Mauthner, F., Fischer, S., Giovannetti, F. and Jakob, K., 2015. "Overheating prevention and stagnation handling in solar process heat applications Authors :".

Halabi, M.A., Al-Qattan, A. and Al-Otaibi, A., 2015. "Application of solar energy in the oil industry — Current status and future prospects". *Renewable and Sustainable Energy Reviews*. ISSN 1364-0321.

Idelchik, I.E., 2008. *Handbook of Hydraulic Resistance*. Begell House, Moscow, 4th edition. ISBN 978-1-56700-340-6.

IEA, 2019. "World energy balances: An Overview". ISSN 1098-6596. doi:10.1017/CBO9781107415324.004. URL https://www.iea.org/reports/world-energy-balances-2019.

Kelly, B. and Kearney, D., 2006. "Parabolic Trough Solar System Piping Model: Final Report". , No. July, p. Size: 23. URL http://www.osti.gov/energycitations/servlets/purl/887341-l7WyHA/%5Cn10.2172/887341.

Lemos, L.F.L., Starke, A.R.A., Boland, J., Cardemil, J.M.J., Machado, R.D.R. and Colle, S., 2017. "Assessment of solar radiation components in Brazil using the BRL model". *Renewable Energy*, Vol. 108. doi:10.1016/j.renene.2017.02.077.

Liu, B., Sun, W., Liu, C. and Guo, L., 2015. "The Thermodynamic Model on Paraffin Wax Deposition Prediction". , No. December, pp. 827–832.

Louvet, Y., Fischer, S., Furbo, S., Giovanetti, F., Mauthner, F., Mugnier, D. and Philippen, D., 2017. "LCOH for Solar Thermal Applications". pp. 1–5. URL http://task54.iea-shc.org/.

Mauthner, F. and Herkel, S., 2016. "Technical Report Subtask C – Part C1". Vol. 2016, No. January, pp. 1–31.

Nguyen, D.A., Fogler, H.S. and Chavadej, S., 2001. "Fused chemical reactions. 2. Encapsulation: Application to remediation of paraffin plugged pipelines". *Industrial and Engineering Chemistry Research*, Vol. 40, No. 23, pp. 5058–5065. ISSN 08885885. doi:10.1021/ie0009886.

OPEC, 2016. "World Oil Outlook 2016". Technical report, OPEC.

Palermo, L.C.M., Souza Jr, N.F., Louzada, H.F., Bezerra, M.C.M., Ferreira, L.S. and Lucas, E.F., 2014. "Development of Multifunctional Formulations for Inhibition of Waxes and Asphaltenes Deposition". *Brazilian Journal of Petroleum and Gas*, Vol. 7, No. 4, pp. 181–192. ISSN 19820593. doi:10.5419/bjpg2013-0015.

Rocha, K., Gutierrez, M.B.G.P.S. and Hauser, P., 2012. "A Remuneracao dos Investimentos em Energia Renovavel no Brasil - Uma Proposta Metodológica ao Benchmark da UNFCCC para o Brasil". Technical report.

Singh, P., Venkatesan, R. and Fogler, H.S., 2000. "Formation and Aging of Incipient Thin Film Wax-Oil Gels". Vol. 46, No. 5, pp. 1059–1074.

Solar Payback, 2018. *Energia Termossolar Para a Indústria - Brasil*. URL https://www.solarwirtschaft.de/fileadmin/user_upload/national_process_heat_mex_spb.pdf.

Starke, A.R., Cardemil, J.M., Escobar, R. and Colle, S., 2017. "Thermal analysis of solar-assisted heat pumps for swimming pool heating". *Journal of the Brazilian Society of Mechanical Sciences and Engineering*, Vol. 39, No. 6, pp. 2289–2306. ISSN 18063691. doi:10.1007/s40430-016-0671-y.

TESS, 2012a. *TESSLibs 17 – Hydronics Library Mathematical Reference*.

TESS, 2012b. *TESSLibs 17 – Solar Library Mathematical Reference*.

TESS, 2014. *TESSLibs 17 – Storage Tank Library Mathematical Reference*.

United Nations, 2012. "Sustainable Energy for All". *A Vision Statement. New York, United Nations*, , No. April, p. 32.

Venkatesan, R., Nagarajan, N.R., Paso, K., Yi, Y., Sastry, A.M. and Fogler, H.S., 2005. "The strength of paraffin gels formed under static and flow conditions". Vol. 60, pp. 3587–3598. doi:10.1016/j.ces.2005.02.045.

Wagner, M. and Gilman, P., 2010. "Technical Manual for the Physical Trough Model". *National Renewable Energy Laboratory*, , No. June.

8. RESPONSIBILITY NOTICE

The authors are solely responsible for the printed material included in this paper.